

# Design and Simulation of a Pressure Sensor Based on Optical Waveguides for Applications in Hydraulic Fracturing

Roberto Ambrosio, Gustavo Lara, Abimael Jimenez,  
Jose Mireles and Juan Ibarra  
Electrical and Computer Engineering Department  
Universidad Autónoma de Ciudad Juárez, UACJ  
Ciudad Juárez, Mexico  
e-mail: rambrosi@uacj.mx

Aurelio Heredia  
Mechatronic and Bioengineering Department  
Universidad UPAEP  
Puebla, Mexico  
e-mail: aureliohoracio.heredia@upaep.mx

**Abstract**— In this work is presented the design and simulation of a pressure sensor for a high range from 4MPa to 83MPa. The purpose is to use Mach-Zehnder Interferometer (MZI) and optical waveguides for applications where corrosion and high temperature levels (up to 120° Celsius) are present. The sensor is designed for down-hole applications like petroleum wells.

**Keywords**—Pressure; sensor; interferometer; waveguide

## I. INTRODUCTION

Hydraulic induced fracturing (HIF) in oil wells is used to increase oil productivity by making the subterranean terrain more deep and permeable. The most important down hole measurements required during hydraulic fracturing are pressure and temperature in first place, and density and viscosity in second place [1].

The conditions in the bottom of the well such as: temperatures of  $\sim 125^{\circ}\text{C}$ , pressures up to 12,000 psi, high shock impacts and corrosive fluids are extreme to some electronics devices.

In order to address the problem of HIF, one possible solution is MOEMS (Micro Opto-Electro-Mechanical Systems) technology, using interferometry techniques with integrated optics (IO). The Si technology in conjunction with techniques of micromachining has enabled the creation of a variety of novel functions MOEMS and IO devices. These systems have integrated sensors and read-out electronic circuits in order to form smart systems [2-4]. The use of photons for sensing has a great field of possibilities to be measured such as: intensity, wavelength, phase and polarization. Also photons present many advantages such as: remote interrogation, freedom of electromagnetic interferences, multiplexed detection, and availability of well established technology from communications industry: e.g. lasers, detector arrays and waveguides [5-6]. Among various types of functional IO devices, an interferometer is one of the most important and used elements. Interferometry has been widely adopted for

pressure sensing due to its high sensitivity and compatibility with Si technology [4, 5]. Integrated optical interferometers based on the Mach-Zehnder configuration seems to be the most employed due to its simplicity in design and fabrication. Waveguide devices based on Mach-Zehnder interferometer (MZI) configurations have been used in applications such as switches/modulators [7, 8] and sensors with low pressure ranges [9]. In this work is studied the proposal for using a MZI sensor in HIF for a high range of pressure; taking on of the advantages of the sensor scheme is the use of a source of light (HeNe laser,  $\lambda=632.8\text{nm}$ ) and the signal conditioning can be outside of the downhole, while the sensor is inside, therefore this MOEMS is passive, and making it able to be used for extreme conditions, the simulations were carried out by software COMSOL multiphysics 4.0.

## II. DEVICE STRUCTURE

The fig. 1 shows the schema for the propose sensor based in MZI, it is composed by an optical waveguide, which has two

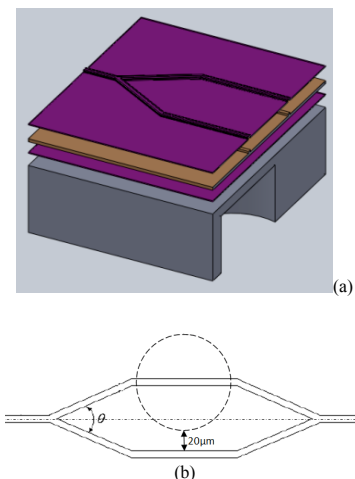


Figure 1. a) Extruded layers of MZI and b) detail of the sensing area

arms, one is over a circular micromachined membrane and it is the sensing region and the other is the reference arm (see Figure 1a and 1b). In this structure the beam light is transmitted through an optical fiber, which is carefully assembled and connected to a (substrate/core/cladding) waveguide, where the core has the highest refractive index. The membrane is deflected due to the applied pressure then the refractive index of the waveguide changes and also the phase of the light.

The material properties using in the simulation are listed in table 1. The device structure is composed by: silicon dioxide silicon nitride, and silicon as substrate

### A. Design

The waveguide selected is the rib waveguide (see Fig. 2), between four types, (embossed waveguide, rib waveguide, waveguide embedded line, and line wave-guide) due to low cost of fabrication, and the electromagnetic wave is confined in the center of the waveguide geometry. The rib waveguide geometrical conditions for single mode propagation are the following (1) [10]:

$$\frac{a}{b} \leq \frac{r}{\sqrt{1-r^2}} \quad (1)$$

$$0.5 \leq r < 1$$

Selecting the following values:  $r=0.6$  at  $632.8\text{nm}$ , results  $2\lambda a=1\mu\text{m}$ ,  $2\lambda b=1.5\mu\text{m}$ ,  $2\lambda br=0.9\mu\text{m}$ . To obtain the effective refractive index, it was simulated taking in account the cross section of the optical waveguide. From (2) [11], the membrane was designed considering the weakest material of the device, which is the silicon with 7GPa of yield point

$$w_c = \frac{3Pr^4}{16Eh^3}(1-\nu^2) \quad (2)$$

where  $w_c$  is the maximum displacement,  $P$  is the pressure,  $E$  is the Youngs module,  $\nu$  is Poisson, and  $h$  is the thickness of the membrane,  $h$  can be calculated from (3)

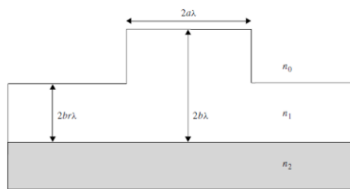


Figure 2. Geometrical conditions for a single mode rib waveguide

TABLE I. MATERIAL PROPERTIES

Properties	Si	SiO <sub>2</sub>	Si <sub>3</sub> N <sub>4</sub>
Density (g/cm <sup>3</sup> )	2.4	2.2	2.9-3.1
Young's modulus (GPa)	165	87	323
Thermal conductivity (W/cm <sup>2</sup> *K)	157	0.014	0.19
Poisson ratio	0.3	0.17	0.25
Melting point (°C)	1415	1700	1800
Yield point (GPa)	7	8.4	14
Refractive index	3.44	1.45	2.05
Temperature dependence, n (k <sup>-1</sup> )	2x10 <sup>-4</sup>	1x10 <sup>-5</sup>	-
Thermal expansion (10 <sup>-6</sup> /°C)	2.6	0.5	1.6
Band gap energy (eV)	1.12	~9	~5
Realtive permittivity (ε <sub>r</sub> )	11.7	3.9	4-8

$$h = \sqrt{\frac{3Wv}{4\pi\sigma}} \quad (3)$$

where

$$W=(\pi a^2)P, \quad (4)$$

$a$  is the diameter of the membrane and  $\sigma$  is maximum stress. The propose structure has a diameter of  $150\mu\text{m}$ , the membrane is designed considering the maximum pressure, with a calculated thickness equal to  $3.9\mu\text{m}$

### III. SIMULATION RESULTS

Fig. 3 shows the electromagnetic wave confinement in the waveguide and the effective refractive index of the material, which is approximately to the theoretical value.

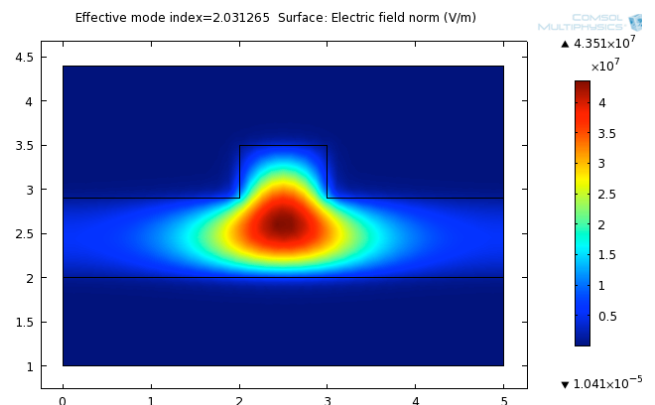
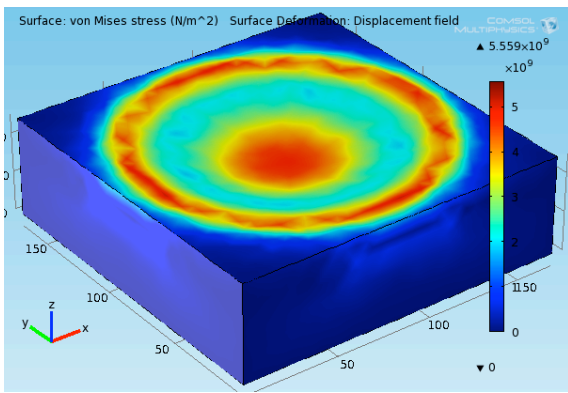
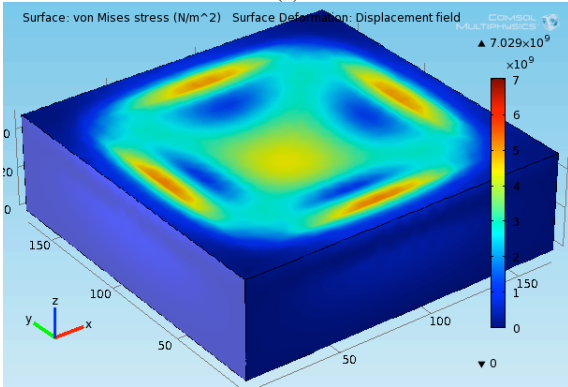


Figure 3. Effective refractive index of the structure



(a)



(b)

Figure 4. Comparison of stress and displacement for two types of membrane: (a) circular and (b) square

In Fig. 4 is showed a comparison of two shapes of membrane: circular and square, using the same area for both, the circular membrane presented the most displacement and the less stress than the square membrane, thus in a circular membrane is the best option for type of applications due to the stress is more distributed in the perimeter and hence can be applied a high pressure.

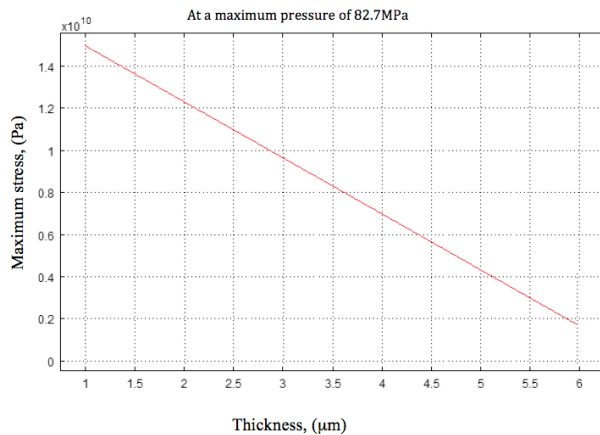


Figure 5. Stress as a function of thickness of the membrane

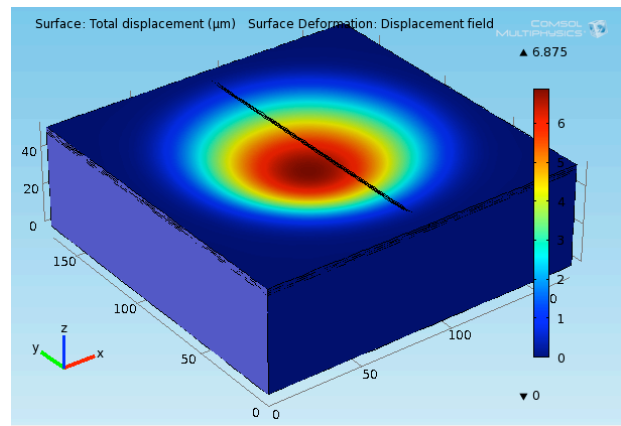


Figure 6. Total displacement on the sensing area

Fig. 5 shows the maximum stress at 82.7 MPa of pressure, from this simulation the thickness of the micromachined membrane can be select, for example in the plot at 4 μm the stress is approximately 6 GPa; therefore taking in account the yield point of the silicon material, 5 μm of thickness is enough for our design.

In Fig. 6 is represented the distribution for the displacement when the maximum pressure is applied to the design structure using a thickness of the 5 μm.

The elongation of the waveguide is an important parameter for the transduction, because from it is calculated the phase shift. In Fig. 7 is plotted the phase shift as a function of pressure, for this plot was used 0.6 μm of elongation (ΔL) and the maximum displacement at 100 MPa. Then the design structure showed a sensitivity of 0.26 μrad/Pa.

Finally, in order to study the effect of the temperature in the MZI device, different simulations were performed, in Fig. 8 is showed the displacement of the membrane versus the length arc of the sensing area for a range from 50 to 195 °C and using

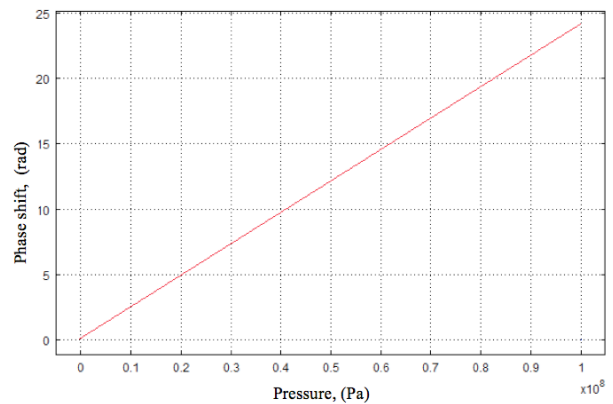


Figure 7. Pressure vs Phase shift relation

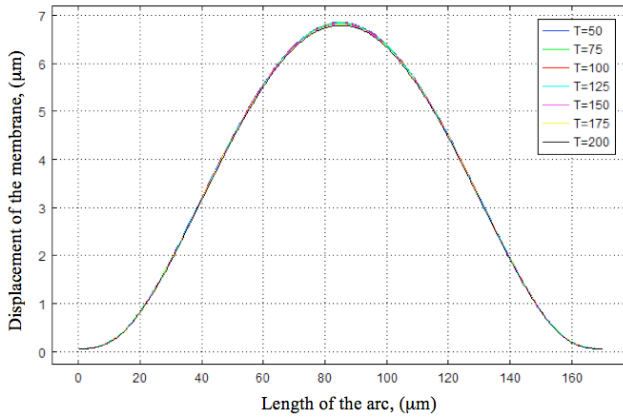


Figure 8. Membrane displacement of the sensing area as a function of temperature

the maximum pressure, from the graph is observed that the temperature practically has no affect significantly the displacement and hence the sensitivity.

#### IV. CONCLUSIONS

In this work a pressure sensor MOEMS have been analyzed and simulated with a configuration of MZI based on waveguide with a circular shape of the sensing area of micromachined membrane. The proposal device is for a wide range of pressure and it is very promising for HIF applications where high pressures and temperature involved this type of sensing.

#### ACKNOWLEDGMENT

The authors want to acknowledge the CONACyT which is the sponsor for the science and technology program of the Mexican government.

- [1] J. Mireles, Jr., H. Estrada and R. C. Ambrosio, "Sensors for hydraulic-induced fracturing characterization", Proc. SPIE 8031, pp. 80311G, 2011.
- [2] D. Wagner, J. Frankenberger and P. Deimel, "Optical pressure sensor using two Mach-Zehnder interferometers for the TE and TM polarization", Journal of Micromech. Microeng., vol. 4, pp. 35-39, 2008
- [3] G. Yixian, M. Wang, X. Chen and H. Rong, "An optical MEMS pressure sensor based on a phase demodulation method". Sensor and actuator A, vol. 143, pp. 224-229, 1994.
- [4] H. Porte, V. Gorel, S. Kiryenko, J. Goedgebuer, W. Daniau, P. Blind, "Imbalanced Mach-Zehnder Interferometer Integrated in Micromachined Silicon Substrate for Pressure Sensor", J. Lighthwave Technol., vol. 17, n. 2, pp. 229-233, 1999.
- [5] K. Benaissa and A. Nathan, "IC compatible opto-mechanical pressure sensor using Mach-Zehnder interferometry", IEEE Trans. Electron Devices, vol.43, no. 9, pp.1571-1581, 1996.
- [6] N. Daldosso, M. Melchiorri, F. Riboli, M. Girardini, G. Pucker, M. Crivellari, P. Bellutti, A. Lui, and L. Pavesi, "Comparison among various  $\text{Si}_3\text{N}_4$  waveguide geometries grown within a CMOS fabrication pilot line", J. of lightwave tech. vol. 22, pp. 1734-1740, 2004.
- [7] J. Gander, J. S. Barton, R. L. Reuben, J. Jones, R. Stevens, K. Chana, S. Anderson, "Embedded Micromachined Fiber-Optic Fabry-Perot Pressure Sensors in Aerodynamics Applications", J. Sensor, 2, vol. 3., pp. 102-107, 2003.
- [8] W. Pulliam, P. M. Russler, and R. S. Fielder, "High-temperature high-bandwidth fiber optic MEMS pressure-sensor technology for turbine engine component testing," Proc. SPIE: Fiber Optic Sensor Technology and Applications 2001, vol. 4578, pp. 229-238, 2002..
- [9] W.P Eaton and J.H Smith, "Micromachined pressure sensors: review and recent developments", J. of Smart materials and structures, vol.6, pp.530-539, 1997.
- [10] Graham T. Reed, Andrew P Knights, Silicon Photonics: An Introduction. John Wiley & Sons Ltd, 2004.
- [11] Zappe, Hanz. Fundamentals of Micro-Optics. Cambridge : Cambridge University Press, 2010